ISSN:3007-9640 DOI: https://doi.org/10.70114/acmsr.2025.3.1.P110

Mechanistic Study of Al/Ga Doping Effects on NCM811 Surface Stability

Zhiyong Chen [1, a], Piqiang Tan [1, a] *, Xiang Liu [1, a], Chaojie Yao [1, a]

[1] School of Automotive Studies, Tongji University, Shanghai, 201804, China.

[a] tanpq@hotmail.com

Abstract. Lithium-ion batteries have emerged as a pivotal technology in green energy storage systems, with their development progressing at an accelerated pace. Within this field, cathode materials represent a critical research frontier as they fundamentally determine the energy density and overall performance of lithium-ion batteries. This study focuses on NCM811, a promising high-nickel cathode material, investigating its surface stability through elemental doping strategies. We systematically examine the exposed crystal surfaces and oxygen vacancy formation energetics modified by dopant incorporation. Furthermore, through detailed electronic structure analysis, we elucidate the fundamental mechanisms by which dopant elements influence material stability. These findings provide significant advancements to the existing body of knowledge on NCM811 cathode materials. Our findings provide valuable complementary insights to the existing body of knowledge regarding NCM811 cathode materials.

Keywords: NCM811; doped; Mechanistic; surface stability.

1. Introduction

With the global exploitation of fossil fuels, climate change and environmental pollution have become increasingly severe.[1] As a green and sustainable alternative, new energy vehicles (NEVs) have emerged as a key solution for achieving the dual-carbon strategy in the transportation sector.[2] The core of NEVs lies in rechargeable lithium-ion batteries, where performance (particularly energy density), is largely determined by the cathode material.[3, 4] Among various options, nickel-cobalt-manganese (NCM) ternary materials stand out due to their high energy density, long cycle life, and cost-effectiveness.[5] By optimizing the Ni-Co-Mn ratio, researchers can tailor these materials to achieve an optimal balance between energy density and thermal stability. It is well established that increasing the Ni content in NCM electrodes enhances their energy density, but this improvement is often accompanied by a decline in structural thermal stability.[6] To achieve both high energy density and structural stability, optimization strategies such as doping and surface coating are essential.[7, 8]

Currently, numerous studies have employed doping strategies to modify NCM electrodes across various compositional systems. Zheng et al. synthesized nanoscale NCM111 via high-temperature solid-state sintering and enhanced its conductivity and structural stability by incorporating tungsten (W), achieving a high specific capacity of 131.9 mAh g^{-1} at an ultrahigh rate of 20 C.[9] Huang et al. demonstrated that modifying NCM523 with Al_2O_3 and graphene sheets significantly improved electrochemical performance, retaining 76.9% capacity after 400 cycles at 3 C.[10] Meanwhile, Pan et al. designed an NCM811 cathode with a spinel mortise-and-tenon structure, which effectively suppressed detrimental volume changes during cycling. Computational and experimental results confirmed its exceptional cyclability, with 82.2% capacity retention after 1,200 cycles at 1 C.[11] Furthermore, we systematically evaluated 39 potential doping elements using density functional theory (DFT) calculations, ultimately identifying Al and Ga as optimal dopants, which were subsequently validated through experimental studies.[12]

In this study, we systematically investigated the exposed surfaces of $LiNiO_2$ using DFT calculations. After identifying the most stable surface configuration, we thoroughly explored the properties of Al- and Ga-doped NCM811 materials. Furthermore, the underlying mechanisms for the observed property modifications were elucidated through detailed electronic density of states (DOS) analysis. Our computational approach provides accurate simulations of experimental

ISSN:3007-9640 DOI: https://doi.org/10.70114/acmsr.2025.3.1.P110
scenarios involving Al/Ga-doped NCM811, thereby offering valuable insights that complement prior theoretical and experimental studies.

2. Computational Detail

The DFT calculations were carried out in the Vienna ab initio simulation package (VASP) based on the plane-wave basis sets with the projector augmented-wave method. The exchange-correlation potential was modeled using the generalized gradient approximation with the Perdew-Burke-Ernzerh of functional.[13, 14] A vacuum region of about 15 Å was applied to avoid the z-axis interaction. The energy cutoff was set to be 450 eV. The Brillouin-zone integration was sampled with a Γ-centered Monkhorst-Pack mesh of 1 × 1 × 1. The structures were fully relaxed until the maximum force on each atom was less than 0.03 eV/Å, and the energy convergent standard was 10-5 eV.

The surface energy E_s can be defined as, $E_s = E_{sur} - nE_{bulk}$, where E_{sur} stands for the energy of surface, E_{bulk} stands for the energy of bulk and n stands for the amount of bulk contained in the surface.

The formation energy of O vacancy E_{vac} can be defined as, $E_{vac} = E_2 + E_0 - E_1$, where E_2 stands for the energy of the structure with O vacancy, E_1 is the energy of the primitive structure, E_0 is the energy O atom.

3. Results and Discussion

3.1 Surface Stability Analysis of $LiNiO_2$ Crystallographic Planes

While our previous studies have demonstrated that bulk-phase Al and Ga doping enhances stability by facilitating electron transfer with oxygen atoms, the surface stability of NCM811 under operational battery conditions remains a critical consideration. This necessitates dedicated investigation of surface structural stability to comprehensively evaluate the material's electrochemical performance. To determine the most stable surface configuration of NCM811, we investigated the (003), (104), and (101) surfaces (as shown in Figure 1), which are the most commonly reported orientations in the literature. Due to computational cost considerations, we employed $LiNiO_2$ as a model system for our initial surface stability studies, as the larger supercell sizes required for NCM811 simulations would be prohibitively time-consuming.

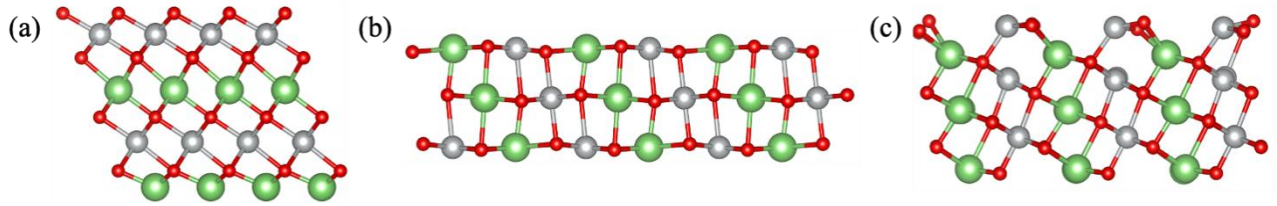

Figure 1. Side view of $LiNiO_2$'s (a) 003, (b) 104 and (c) 101 surfaces.

As shown in Figure 1, all three surfaces ((003), (104), and (101)) exhibit good structural stability with no significant deformation or collapse observed. The calculated surface energies, presented in Figure 2b, reveal that the (104) surface possesses the lowest energy (0.368 J m^{-2}), while the (101) surface shows the highest energy (1.719 J m^{-2}). This energy comparison clearly demonstrates that the (104) surface is thermodynamically the most stable configuration among the three. Consequently, we selected the (104) surface for all subsequent investigations.

ISSN:3007-9640 DOI: https://doi.org/10.70114/acmsr.2025.3.1.P110

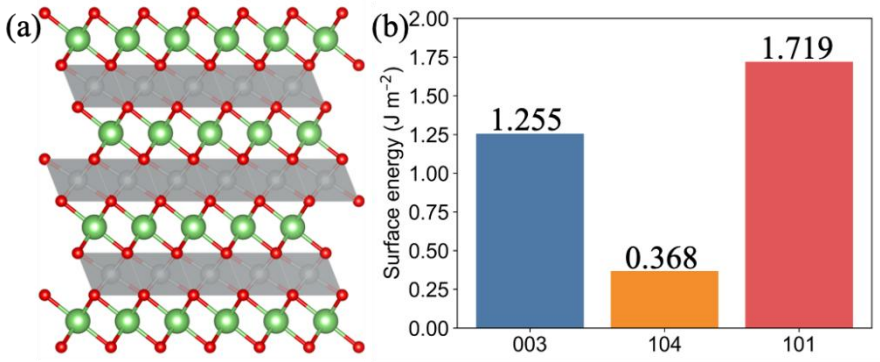

Figure 2. (a) The crystal schematic diagram of LiNiO2, (b) the formation energy of different surface.

3.2 Computational Analysis of Oxygen Vacancy Formation Energy

Using the (104) surface as the base structure, we constructed atomic models of pristine NCM811, Al-doped NCM811, and Ga-doped NCM811. Figure 3a illustrates the specific doping sites for Al/Ga and the corresponding oxygen vacancy locations. Our calculations of oxygen vacancy formation energies for these surface configurations reveal significant differences: the undoped system shows a formation energy of 1.353 eV, while Al- and Ga-doped systems exhibit higher values of 1.882 eV and 1.672 eV, respectively (Figure 3b). These results demonstrate that both Al and Ga doping effectively increase the oxygen vacancy formation energy, indicating that oxygen removal becomes energetically less favorable in doped systems. This enhanced oxygen retention directly correlates with improved structural stability of the cathode material.

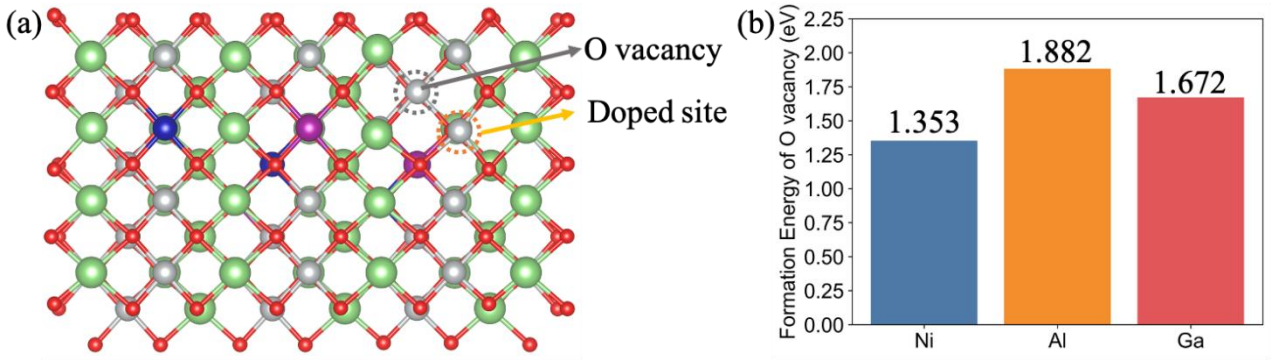

Figure 3. (a) top view of NCM811, Al/Ga doping sites and oxygen vacancy locations, (b) the formation energy of O vacancy of NCM811, Al-doped NCM811 and Ga-doped NCM811.

To elucidate the mechanism behind the enhanced oxygen vacancy formation energy through Al/Ga doping, we performed density of states (DOS) analysis on all three structures prior to oxygen removal (Figure 4). For a detailed electronic structure comparison, we focused specifically on the Al/Ga/Ni dopant sites and their adjacent oxygen atoms (144-O). In the undoped system, partial electron state overlap occurs between Ni and O atoms in the -6.8 eV to Fermi energy range (Figure 3a). However, Ni states primarily concentrate between -6.7 to -4 eV, while O states dominate the -4 to 0 eV range, indicating relatively weak Ni-O bonding. As evidenced by the density of states (DOS) analysis in Figure 4b-c, doping with Al or Ga atoms maintains the characteristic electron concentration region of O atoms within the -4 to 0 eV range. However, the electronic states of the dopants exhibit fundamentally different distributions compared to the original Ni sites. Al 3p electrons primarily concentrate in the -4 to 0 eV range, creating strong orbital overlap with O 2p electrons that effectively stabilizes and contains the O electronic states, resulting in exceptionally strong Al-O bonding. In contrast, Ga 4p electrons display a more uniform distribution across the broader -7 to 0 eV range. While lacking pronounced concentration peaks, the comprehensive coverage of Ga electronic states across the entire O 2p energy region enables stronger Ga-O

ISSN:3007-9640 DOI: https://doi.org/10.70114/acmsr.2025.3.1.P110
bonding compared to the original Ni-O interaction. These distinct electronic configurations explain the enhanced stability observed in both doped systems.

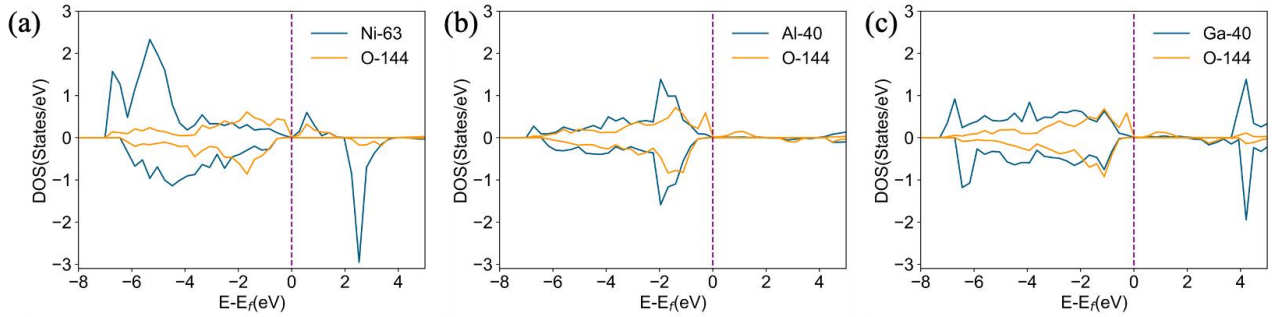

Figure 4. The density of states analysis of (a) NCM811, (b) Al-doped NCM811 and (c) Ga-doped NCM811.

4. Summary

To investigate the dopant effects on surface properties, we conducted comparative studies of pristine, Al-doped, and Ga-doped NCM811 materials. Our systematic investigation proceeded through three key stages: First, we employed density functional theory (DFT) calculations to identify the most stable crystallographic orientation, selecting the (104) plane based on its lowest surface energy. Subsequently, we calculated the oxygen vacancy formation energy for each material system on the (104) surface to quantitatively evaluate how Al and Ga doping enhances structural stability. Finally, through detailed density of states analysis, we elucidated the electronic structure modifications responsible for the observed changes in oxygen vacancy formation energetics.

Acknowledgements

This work was supported by the National Natural Science Foundation of China (No.52076154). The authors would like to thank editors and anonymous reviewers for their suggestions to improve the paper.

References

[1] P. Landrigan, R. Fuller, A. Haines, N. Watts, G. McCarthy, Pollution prevention and climate change mitigation: measuring the health benefits of comprehensive interventions Comment, Lancet Planetary Health, 2018, 2(12): E515-E516.

[2] M. Wu, Z. Li, J. Fan, Selection of new energy vehicles using hybrid approach: A case study of China, Journal of Intelligent & Fuzzy Systems, 2021, 40(6): 11967-11980.

[3] B. Qu, B. Zhang, S. Zheng, Z. Shi, Q. Wu, Progress of four types of cathode materials for lithium-ion batteries, Chinese Journal of Power Sources, 2016, 40(7): 1515-1518,1540.

[4] F. Xiong, W. Zhang, Z. Yang, F. Chen, T. Wang, Z. Chen, Research progress on cathode materials for high energy density lithium ion batteries, Energy Storage Science and Technology, 2018, 7(4): 607-617.

[5] S. Wei, S. Hou, G. Zhou, S. Dong, Y. Hu, J. Wang, Research and prospect on doping modification of high nickel ternary materials, New Chemical Materials, 2023, 51(3): 58-62.

[6] M. Jiang, D.L. Danilov, R.-A. Eichel, P.H.L. Notten, A Review of Degradation Mechanisms and Recent Achievements for Ni-Rich Cathode-Based Li-Ion Batteries, Advanced Energy Materials, 2021, 11(48): 1042.

[7] K.H. Choi, X. Liu, X. Ding, Q. Li, Design strategies for development of nickel-rich ternary lithium-ion battery, Ionics, 2020, 26(3): 1063-1080.

[8] W. Huang, W. Li, M. Gao, X. Wang, J. Wang, W. Zhuang, Integrated Modification Strategy Enables Remarkable Cyclability and Thermal Stability of Ni-Rich Cathode Materials for Lithium-Ion Batteries, Acs Applied Materials & Interfaces, 2022, 14(38): 43085-43094.

ISSN:3007-9640 DOI: https://doi.org/10.70114/acmsr.2025.3.1.P110
[9] P.-y. Li, Y.-d. Huang, L.-b. Tang, H.-x. Wei, H. Fu, Z.-j. He, J.-c. Zheng, W-Doped LiNi1/3Co1/3Mn1/3O2 with Excellent High-Rate Performance Synthesized via Hydrothermal Lithiation, Journal of the Electrochemical Society, 2022, 169(5): 050509.

[10] Y. Huang, Q. Liu, L. Chen, J. Tao, G. Zhao, Y. Chen, J. Li, Y. Lin, Z. Huang, Pathways toward Improved Performance of NCM523 Pouch Cell via Incorporating Low-Cost Al2O3 and Graphene, Acs Applied Energy Materials, 2020, 3(11): 10920-10930.

[11] X. Tan, Z. Chen, T. Liu, Y. Zhang, M. Zhang, S. Li, W. Chu, K. Liu, P. Yang, F. Pan, Imitating Architectural Mortise-Tenon Structure for Stable Ni-Rich Layered Cathodes, Advanced Materials, 2023, 35(32): 2301096.

[12] T. Piqiang, C. Zhiyong, L. Xiang, Y. Chaojie, Stepwise Screening Process for Further Dopant of NCM811 Cathode Material to Enhance the Reliability of Lithium–Ion Batteries, The Journal of Physical Chemistry C, 2025, https://doi.org/10.1021/acs.jpcc.4c08302.

[13] J.P. Perdew, K. Burke, M. Ernzerhof, Generalized gradient approximation made simple (vol 77, pg 3865, 1996), Physical Review Letters, 1997, 78(7): 1396-1396.

[14] n. Perdew, n. Chevary, n. Vosko, n. Jackson, n. Pederson, n. Singh, n. Fiolhais, Atoms, molecules, solids, and surfaces: Applications of the generalized gradient approximation for exchange and correlation, Physical Review B , 1992, 46(11), 6671-6687.